Numerical Simulation of the Crookes Radiometer

Luc Mieussens, Guillaume Dechristé

Institut de Mathématiques de Bordeaux
Université de Bordeaux

Séminaire de mécanique des fluides numériques, Institut Henri Poincaré
January 25–26, 2016

Crookes radiometer

- invented by W. Crookes (1874)

145. The apparatus is shown in fig. 6. It consists of four arms, of very fine glass, passing horizontally through pieces of pith (b), and afterwards bent twice at right angles, as shown in the figure. Through the centre of the pieces of pith (b) is passed vertically the point of a very fine sewing-needle (a), which rests in a glass cup (c) blown on to the end of the glass tube e. At the end of each glass arm is fastened a thin disk of pith, white on one side and lampblacked on the other, the black surfaces of all the disks facing the same way. The whole is enclosed in a glass bulb blown on to the end of a wide tube. f is a piece of cement to keep the support (e) in its place. g is the tube containing cocoanut-shell charcoal; the other end is sealed on to the mercury-pump. The exhaustion is effected as already described (131); and the apparatus is then sealed off, with the char-

Fig. 6.

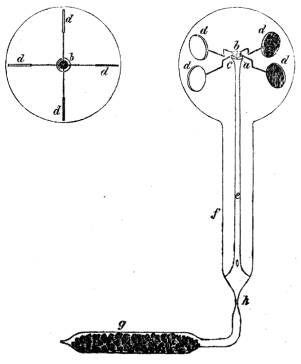

- rarefied gas effect (Kn$\approx$ 0.1): disappears in vacuum or with dense gases
- Reynolds, Maxwell:

light $\rightarrow$ heated vanes

$\rightarrow$ temperature difference in the gas

$\rightarrow$ force (radiometric forces)

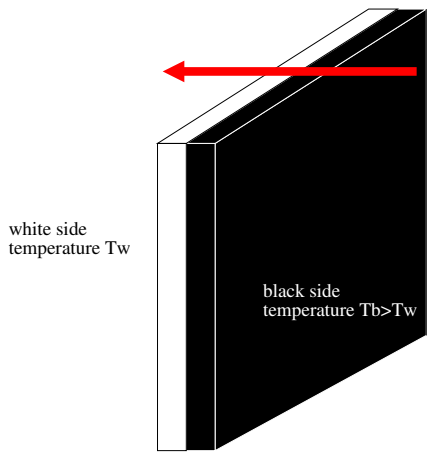

Radiometric forces

- renewed interest: possible application for microflows (MEMS)
- this talk: a numerical tool for 3D simulations of the Crookes radiometer (based on the Boltzmann equation)
- other applications: any rarefied flow with moving obstacles (e.g. vacuum pumps)

Outline

Origin of the radiometric forces

- Crookes: radiation pressure ("radiometer")
- Reynolds 1874: pressure difference in the gas

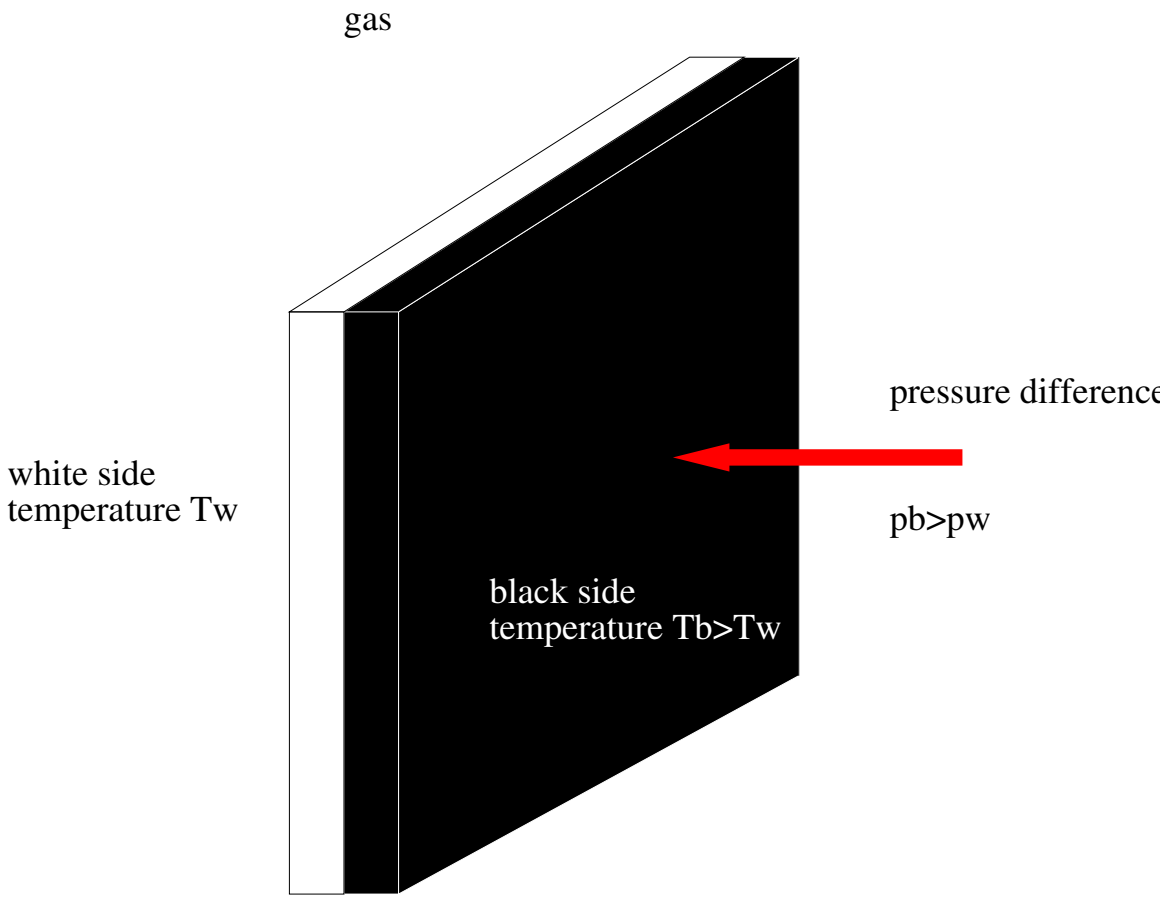

"area" effect

Origin of the radiometric forces

- Reynolds and Maxwell 1879: edge effect

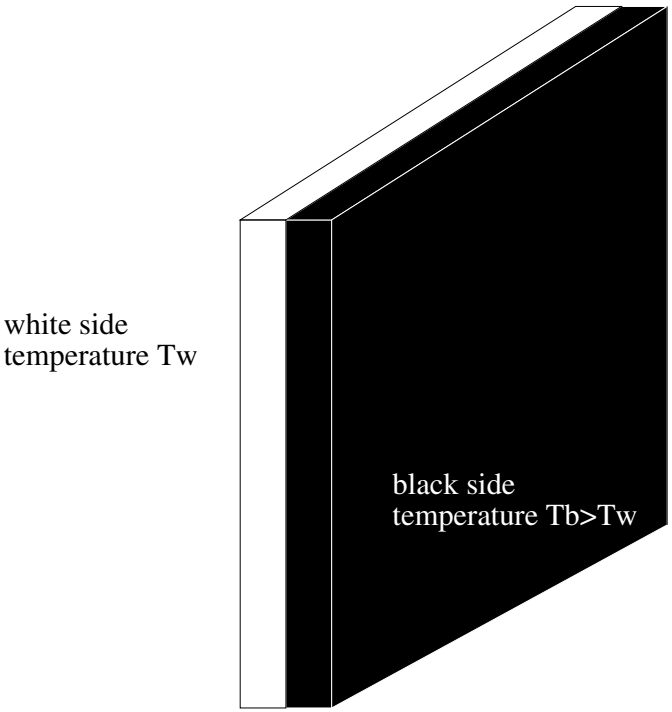

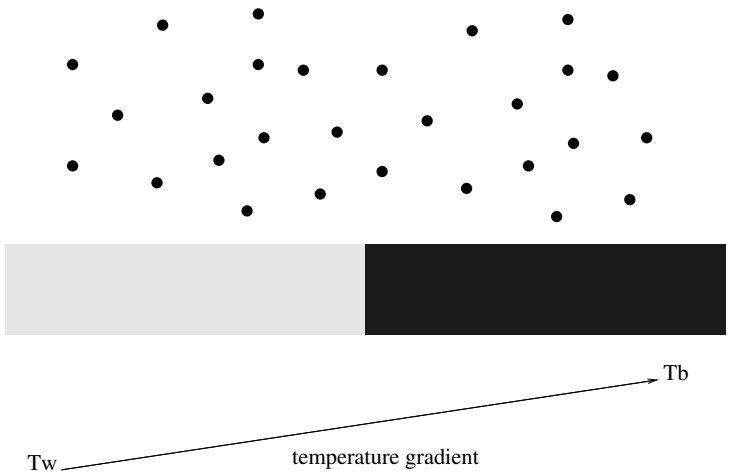

Origin of the radiometric forces

- Reynolds and Maxwell 1879: edge effect

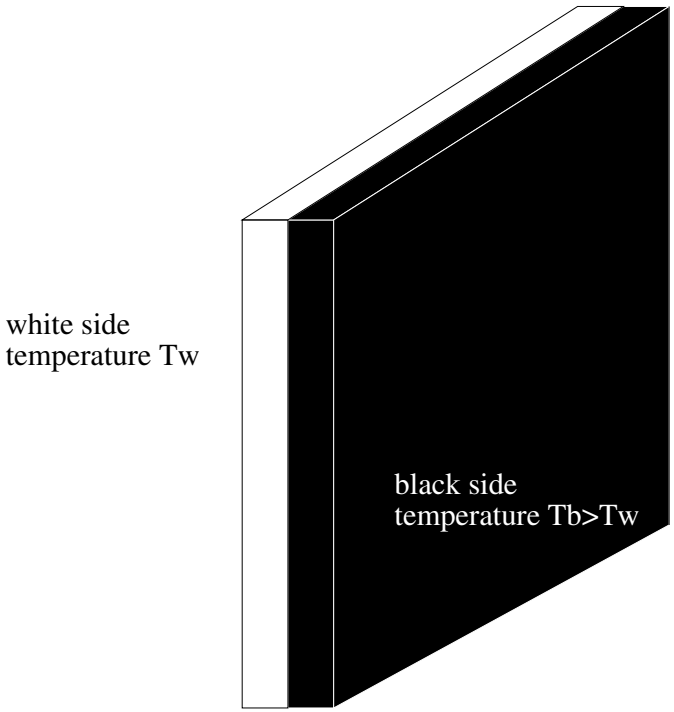

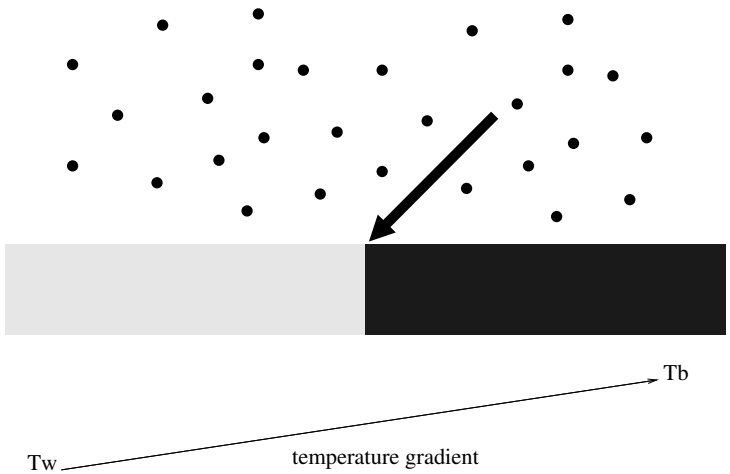

Origin of the radiometric forces

- Reynolds and Maxwell 1879: edge effect

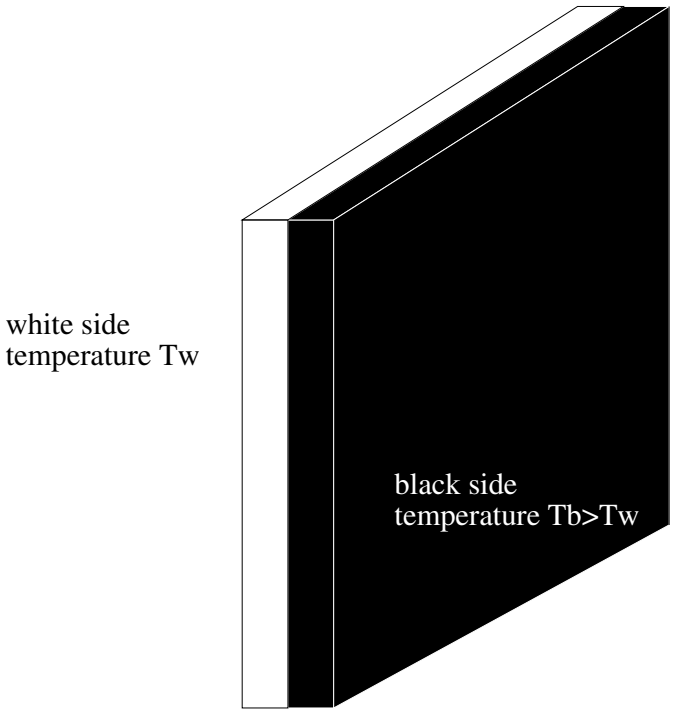

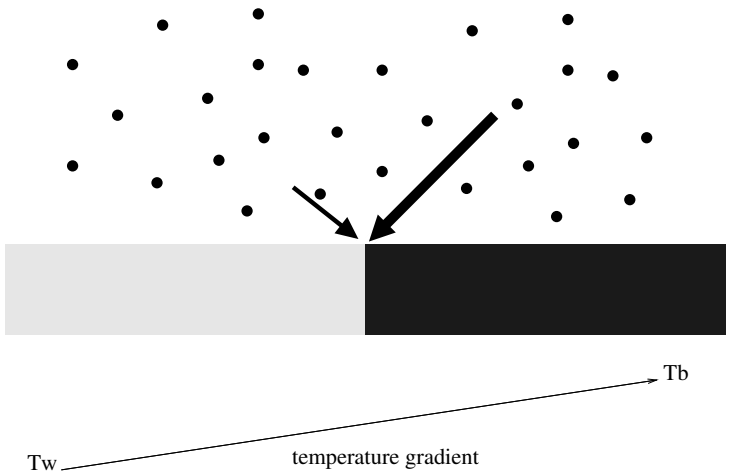

Origin of the radiometric forces

- Reynolds and Maxwell 1879: edge effect

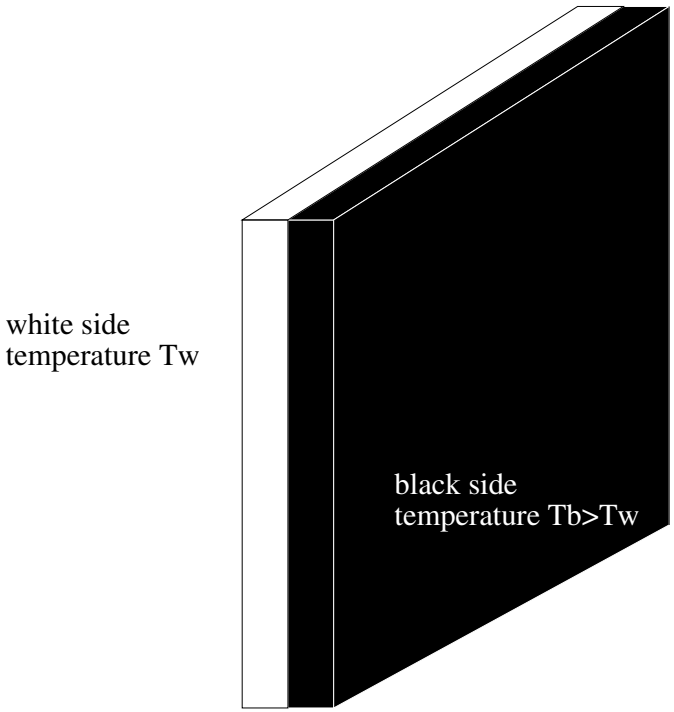

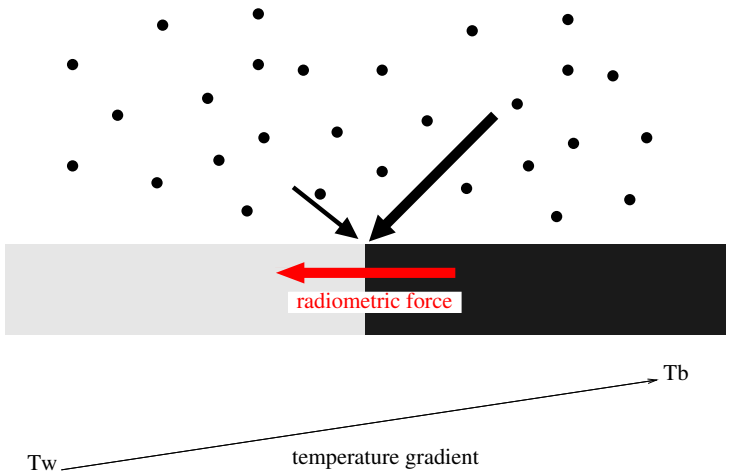

Origin of the radiometric forces

- Reynolds and Maxwell 1879: edge effect

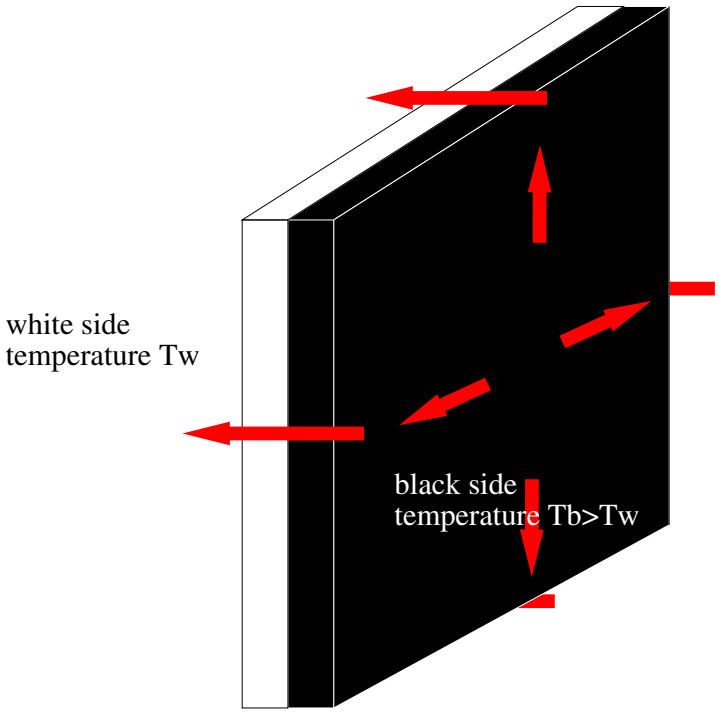

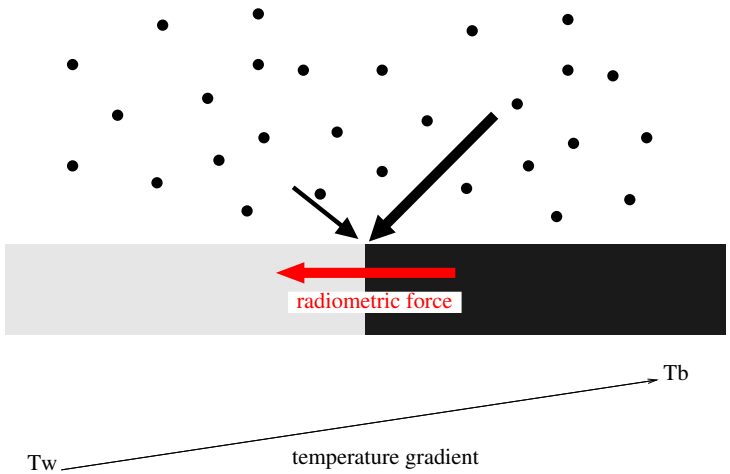

Origin of the radiometric forces

- recent works:
  - Gimelshein, Muntz, Selden, Ketsdever, Alexeenko, etc. (2009 to 2012): numerical and experimental studies (single vane, steady 2D flow)
  - Aoki-Taguchi 2012: numerical studies (investigation of various thermally induced flows, single vane, steady 2D flow)
  - K. Xu 2012 : numerical simulation of a 2D Crookes radiometer
- only 2D simulations, few experiments
- still open questions:
  - 3D flow structure not known (lack of experiments)
  - what is the optimal shape of the vanes?
  - what is the distribution of forces on the vanes?

Boltzmann equation

- particles: position $\vec{x}$ and velocity $\vec{v}$
- mass density in phase-space $f(t, \vec{x}, \vec{v})$ ("Distribution function"): $f(t, \vec{x}, \vec{v})dxdv$ is the mass of particles at $x \pm dx$ with velocity $v \pm dv$.
- Macroscopic quantities:

$$\begin{pmatrix} \rho \\ \rho\vec{u} \\ E \end{pmatrix} = \int_{\mathbb{R}^3} \begin{pmatrix} 1 \\ \vec{v} \\ \frac{1}{2}\|\vec{v}\|^2 \end{pmatrix} f(t, \vec{x}, \vec{v}) d\vec{v}$$

$$\begin{aligned} E &= \frac{1}{2}\|\vec{u}\|^2 + \frac{3}{2}\rho RT \\ P &= \rho RT \end{aligned}$$

Boltzmann equation

- equilibrium distribution ("Maxwellian"):

$$\mathcal{M}[\rho, \vec{u}, T] = \frac{\rho}{(2\pi RT)^{3/2}} \exp\left(\frac{\|\vec{u} - \vec{v}\|^2}{2RT}\right)$$

- important macroscopic quantity here: stress tensor Σ

$$\Sigma(t, \vec{x}) = \int_{\mathbb{R}^3} (\vec{v} - \vec{u}) \otimes (\vec{v} - \vec{u}) f(t, \vec{x}, \vec{v})\, dv$$

- force exerted by the gas on a solid surface dS (of normal $\vec{n}$):

$$F_{gas \to dS} = -\Sigma \vec{n} dS.$$

Boltzmann equation

- Boltzmann equation:

$$\frac{\partial f}{\partial t} + v \cdot \nabla_x f = Q(f)$$

$Q(f)$ is the collision operator

- BGK Model:

$$\frac{\partial f}{\partial t} + v \cdot \nabla_x f = \frac{1}{\tau}(\mathcal{M}[\rho, \vec{u}, T] - f)$$

- consistency with fluid mechanics

Boltzmann equation

- gas-surface interaction: diffuse reflection

  for every reflected velocity,
  i.e v such that $(v - u_w) \cdot n < 0$:

$$f(t,x,v) := \frac{\rho_w}{(2\pi R T_w)^{3/2}} \exp\left(-\frac{|v-u_w|^2}{2RT_w}\right)$$

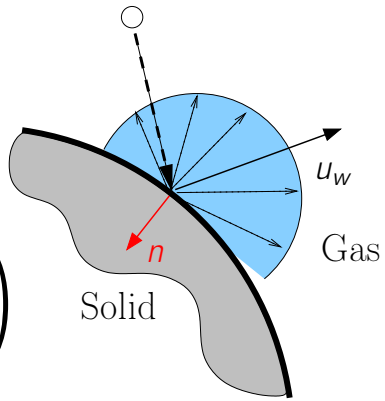

  with ρ_w such that

$$\int_{\mathbb{R}^3} (v - u_w) \cdot n \, f(t,x,v) \, dv = 0$$

  (no mass flux across the wall)

Numerical Method

CFD with moving obstacles:

- body fitted methods with moving grids (ALE, moving mesh)

  e.g. [Chen, Xu, Lee, Cai, 2012].

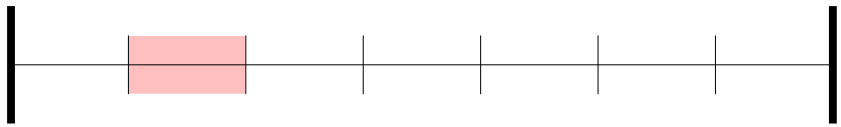

  - ▷ high accuracy at solid boundaries
  - ▷ mesh generation is difficult for complex geometries

Numerical Method

CFD with moving obstacles:

- body fitted methods with moving grids (ALE, moving mesh)

  e.g. [Chen, Xu, Lee, Cai, 2012].

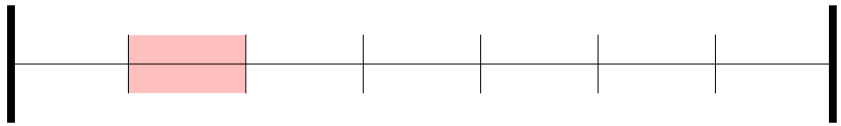

  - ▷ high accuracy at solid boundaries
  - ▷ mesh generation is difficult for complex geometries

- immersed boundary methods e.g. [Filbet Yang 2012], [Perkardan Chigullapalli Alexeenko 2012], [Bernard Iollo Puppo 2014], [Chen Xu 2015]

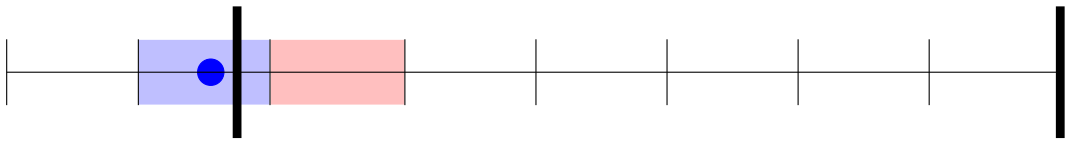

  - ▷ automatic meshing
  - ▷ complex geometries easily handled
  - ▷ low accuracy at solid boundaries : no mass conservation

Numerical Method

- Cut-cell method:

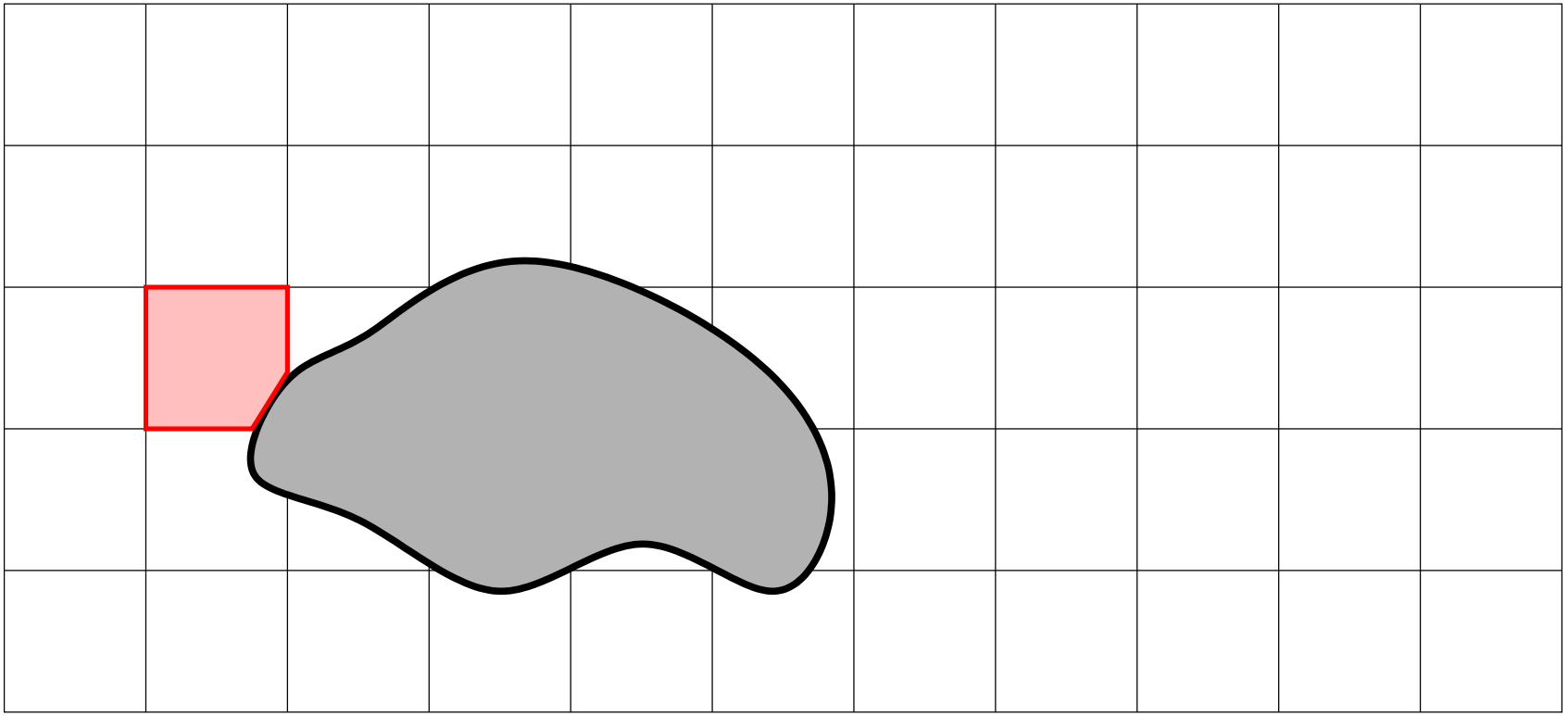

  - Cartesian grid + cut-cells around the solid body
  - complex geometries easily handled
  - potentially good accuracy at solid boundaries (body fitted mesh)

Numerical Method

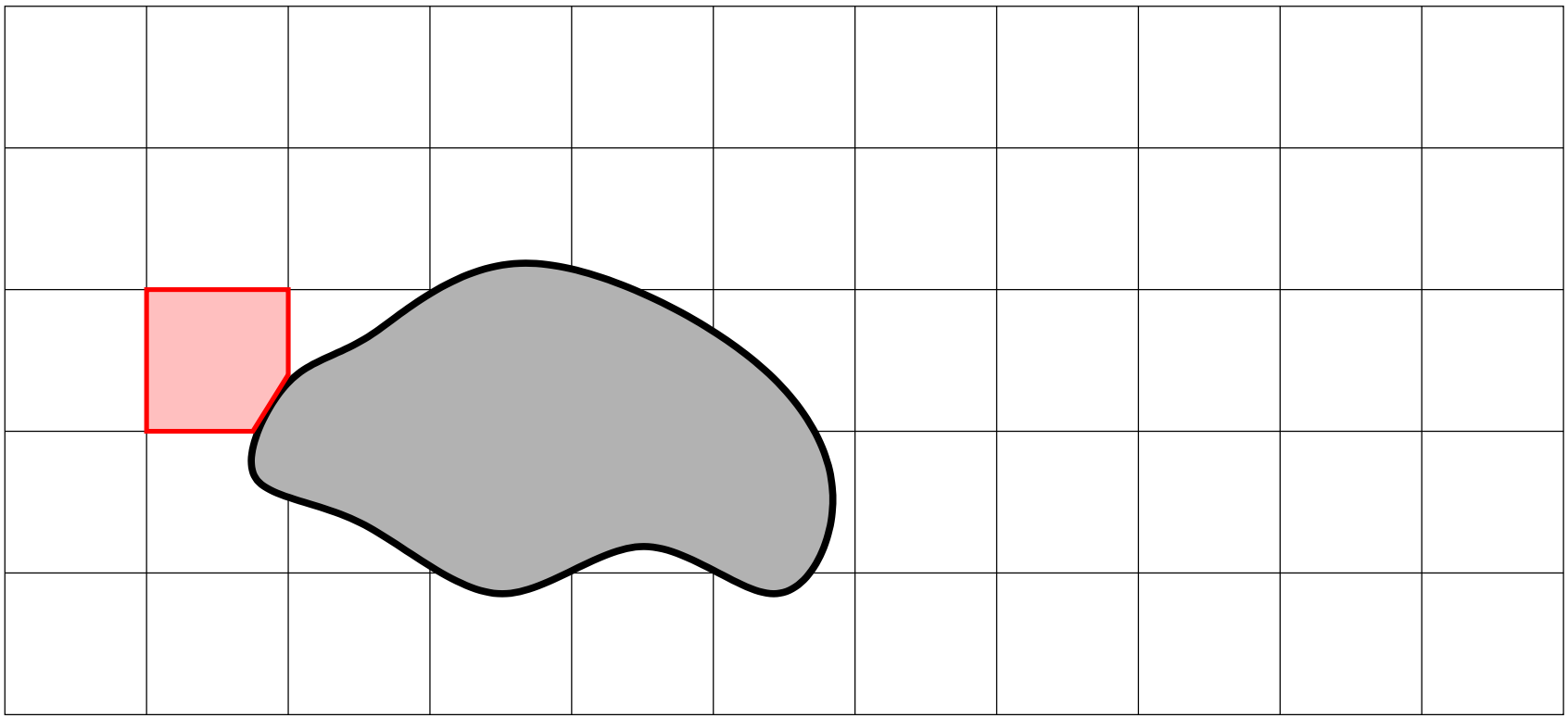

Numerical Method

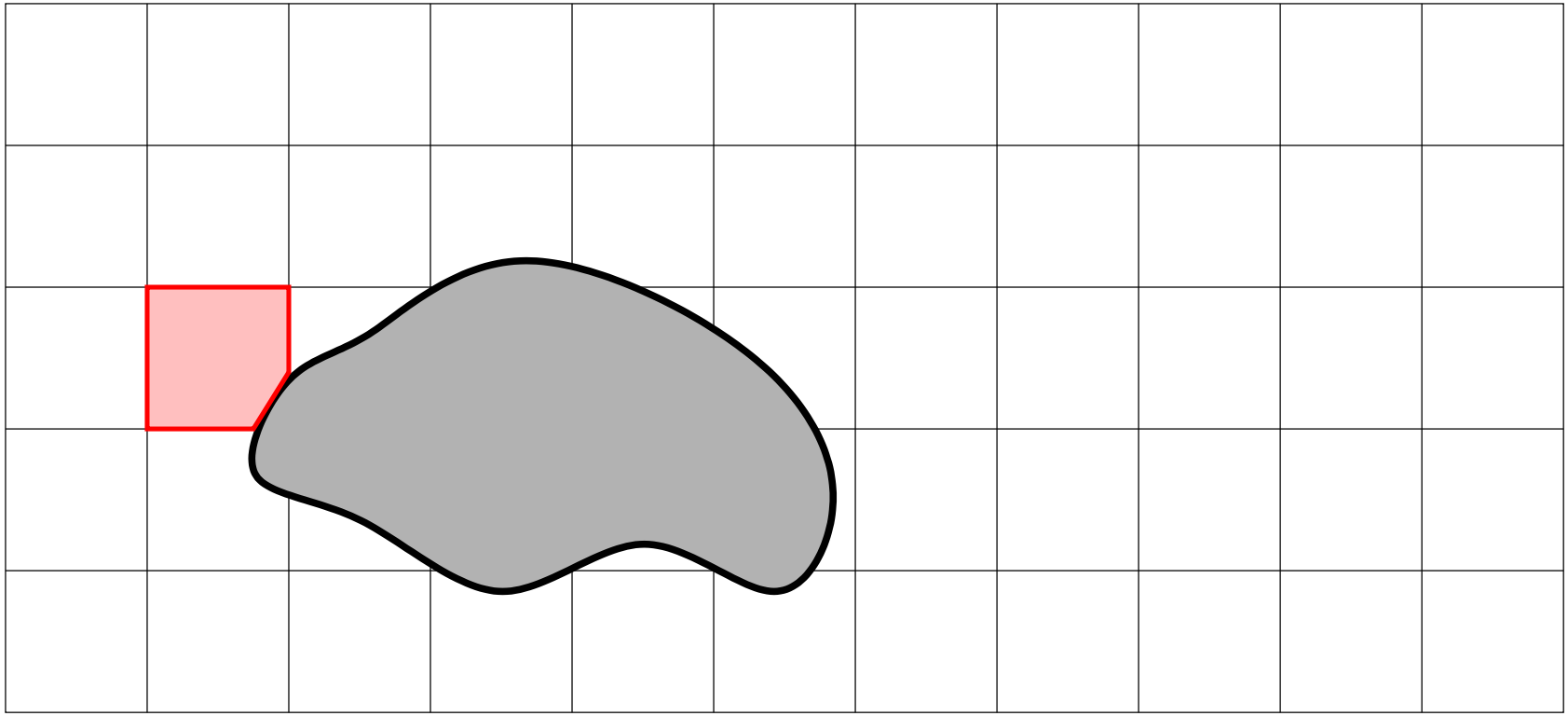

the Boltzmann equation must be solved on changing cells

Basic tools (I): integral formulation

- Boltzmann equation:

$$\frac{\partial}{\partial t} f + v \cdot \nabla_x f = Q(f)$$

- integrate on a time dependent domain $\Omega(t)$

$$\int_{\Omega(t)} \left(\frac{\partial}{\partial t} f + v \cdot \nabla_x f \right) \, dx = \int_{\Omega(t)} Q(f) \, dx.$$

- Stokes formula and Reynolds theorem:

Basic tools (I): integral formulation

- Boltzmann equation:

$$\frac{\partial}{\partial t} f + v \cdot \nabla_x f = Q(f)$$

- integrate on a time dependent domain $\Omega(t)$

$$\int_{\Omega(t)} \left(\frac{\partial}{\partial t} f + v \cdot \nabla_x f \right) \, dx = \int_{\Omega(t)} Q(f) \, dx.$$

- Stokes formula and Reynolds theorem:

$$\int_{\Omega(t)} \frac{\partial}{\partial t} f \, dx + \int_{S(t)} v \cdot n \, f \, dS = \int_{\Omega(t)} Q(f) \, dx.$$

Basic tools (I): integral formulation

- Boltzmann equation:

$$\frac{\partial}{\partial t} f + v \cdot \nabla_x f = Q(f)$$

- integrate on a time dependent domain $\Omega(t)$

$$\int_{\Omega(t)} \left(\frac{\partial}{\partial t} f + v \cdot \nabla_x f \right) \, dx = \int_{\Omega(t)} Q(f) \, dx.$$

- Stokes formula and Reynolds theorem:

$$\frac{\partial}{\partial t} \int_{\Omega(t)} f \, dx - \int_{S(t)} w \cdot n \, f \, dS + \int_{S(t)} v \cdot n \, f \, dS = \int_{\Omega(t)} Q(f) \, dx.$$

Basic tools (I): integral formulation

- Boltzmann equation:

$$\frac{\partial}{\partial t} f + v \cdot \nabla_x f = Q(f)$$

- integrate on a time dependent domain $\Omega(t)$

$$\int_{\Omega(t)} \left(\frac{\partial}{\partial t} f + v \cdot \nabla_x f \right) \, dx = \int_{\Omega(t)} Q(f) \, dx.$$

- Stokes formula and Reynolds theorem:

$$\frac{\partial}{\partial t} \int_{\Omega(t)} f \, dx + \int_{S(t)} (v - w) \cdot n \, f \, dS = \int_{\Omega(t)} Q(f) \, dx.$$

Basic tools (II): finite volume method

- cell average of f on a cell Ω_i^n:

$$f_i^n = \frac{1}{|\Omega_i^n|} \int_{\Omega_i^n} f(t^n, x, v)\, dx$$

- integral equation:

$$\frac{\partial}{\partial t} \int_{\Omega(t)} f\, dx + \int_{S(t)} (v - w) \cdot n\, f\, dS = \int_{\Omega(t)} Q(f)\, dx.$$

  where w is the velocity of the faces of the cell

- first order explicit upwind scheme:

$$|\Omega_i^{n+1}| f_i^{n+1} - |\Omega_i^n| f_i^n + \Delta t \sum_j \mathcal{F}_{ij}^n = \Delta t |\Omega_i^n| Q(f_i^n).$$

Basic tools (II): finite volume method

- first order explicit upwind scheme:

$$|\Omega_i^{n+1}| f_i^{n+1} - |\Omega_i^n| f_i^n + \Delta t \sum_j \mathcal{F}_{ij}^n = \Delta t |\Omega_i^n| Q(f_i^n).$$

- numerical flux between cell Ω_i^n and Ω_j^n:

$$\mathcal{F}_{ij}^n \approx \int_{interface \Omega_i^n / \Omega_j^n} (v - w) \cdot n \, f(t^n, x, v)) \, dS$$

  - for a gas interface: $w = 0$

$$\mathcal{F}_{ij}^n = |S_{ij}^n| \left[(v \cdot n_{ij})^+ f_i^n + (v \cdot n_{ij})^- f_j^n \right]$$

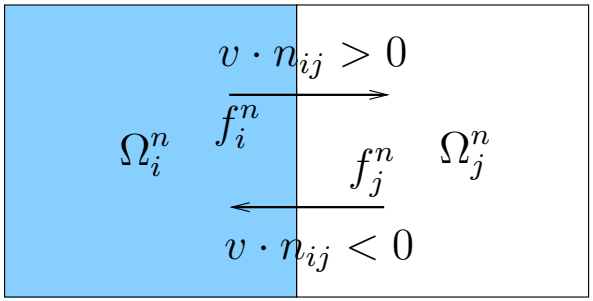

Basic tools (II): finite volume method

- first order explicit upwind scheme:

$$|\Omega_i^{n+1}| f_i^{n+1} - |\Omega_i^n| f_i^n + \Delta t \sum_j \mathcal{F}_{ij}^n = \Delta t |\Omega_i^n| Q(f_i^n).$$

- numerical flux between cell Ω_i^n and Ω_j^n:

$$\mathcal{F}_{ij}^n \approx \int_{interface \Omega_i^n / \Omega_j^n} (v - w) \cdot n \, f(t^n, x, v)) \, dS$$

  - for a solid interface: $w = u_w$ (velocity of the solid wall)

$$\mathcal{F}_{ij}^n = |S_{ij}^n| \left[((v - u_{w,ij}^n) \cdot n_{ij})^+ f_i^n + ((v - u_{w,ij}^n) \cdot n_{ij})^- M[\rho_w, u_w, T_w] \right]$$

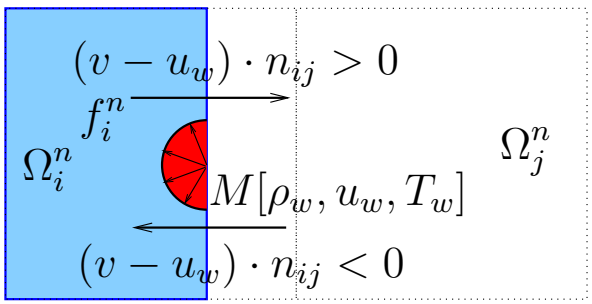

Solid-gas coupling

- at t^n: f_i^n is known for every cell Ω_i^n, velocity $u_{w,i}^n$ of solid nodes as well
- new position of grid nodes at t^{n+1}:

$$x_i^{n+1} = x_i^n + \Delta t \, u_{w,i}^n$$

- this gives new cut cells
- average values f_i^{n+1} on new cells Ω_i^{n+1} are computed with the finite volume scheme
- force and torque exerted by the gas on the solid wall are computed with stress tensor + boundary conditions
- new node velocity $u_{w,i}^{n+1}$ are computed with Newton laws

Technical details (I): small cell problem

- very small cut cells: very small Δt

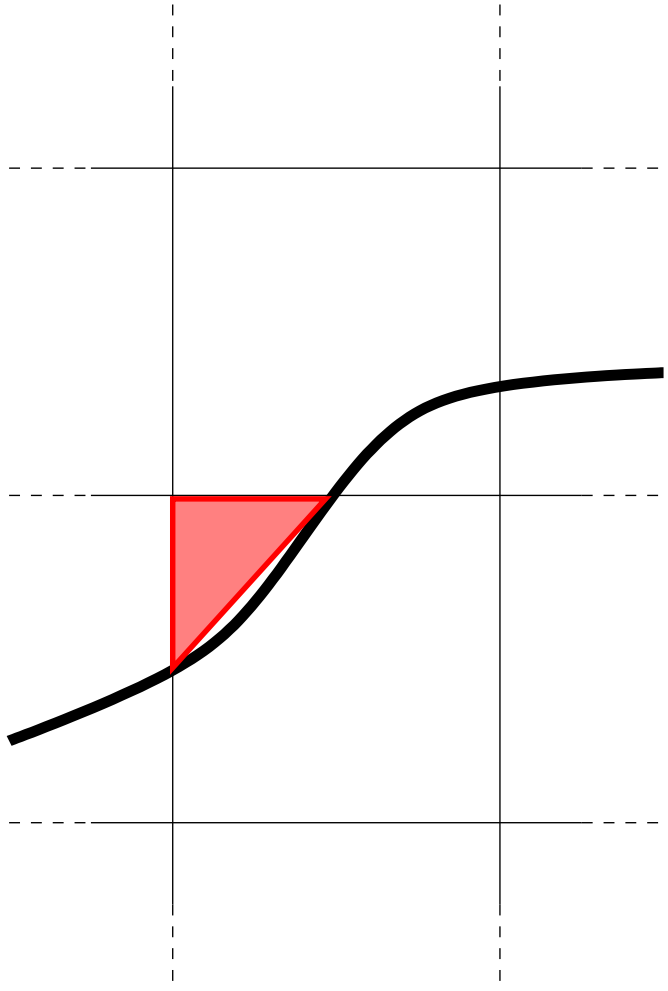

Technical details (I): small cell problem

- very small cut cells: very small Δt
  $\rightarrow$ cells merged in a control volume

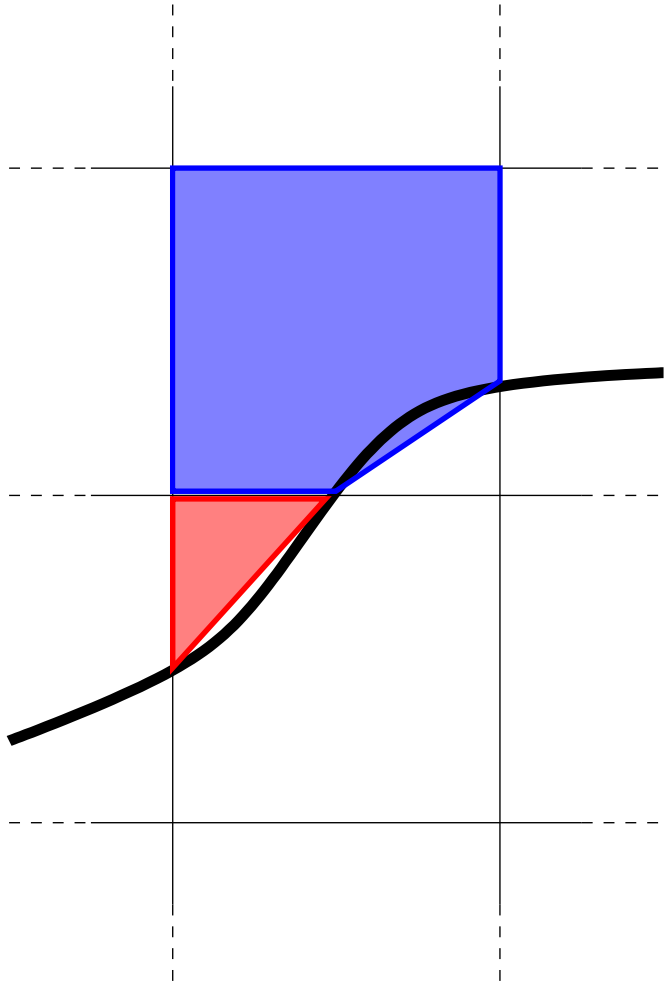

Technical details (I): small cell problem

- very small cut cells: very small Δt
  $\rightarrow$ cells merged in a control volume

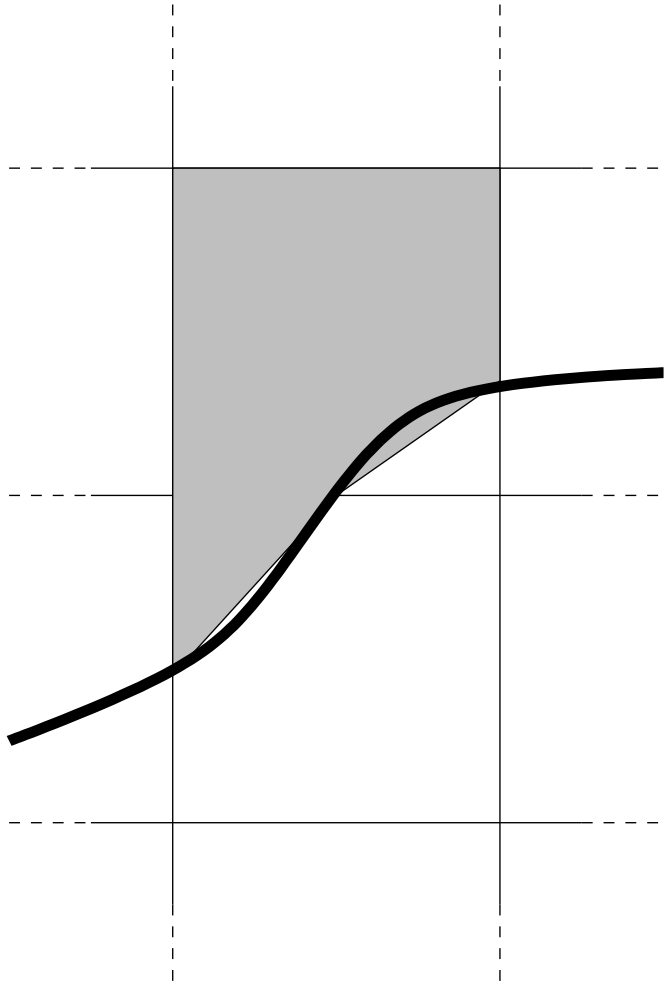

Technical details (I): small cell problem

- very small cut cells: very small Δt
  $\rightarrow$ cells merged in a control volume
- time integration in the control volume

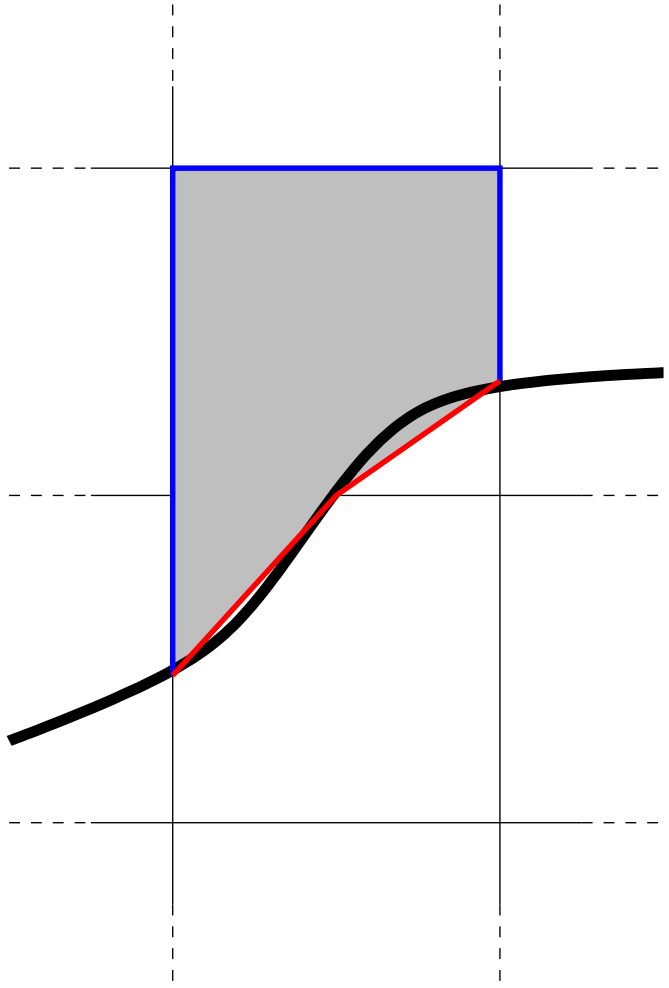

Technical details (I): small cell problem

- very small cut cells: very small Δt
  $\rightarrow$ cells merged in a control volume
- time integration in the control volume
- distribute the gas of the control volume to its cells :

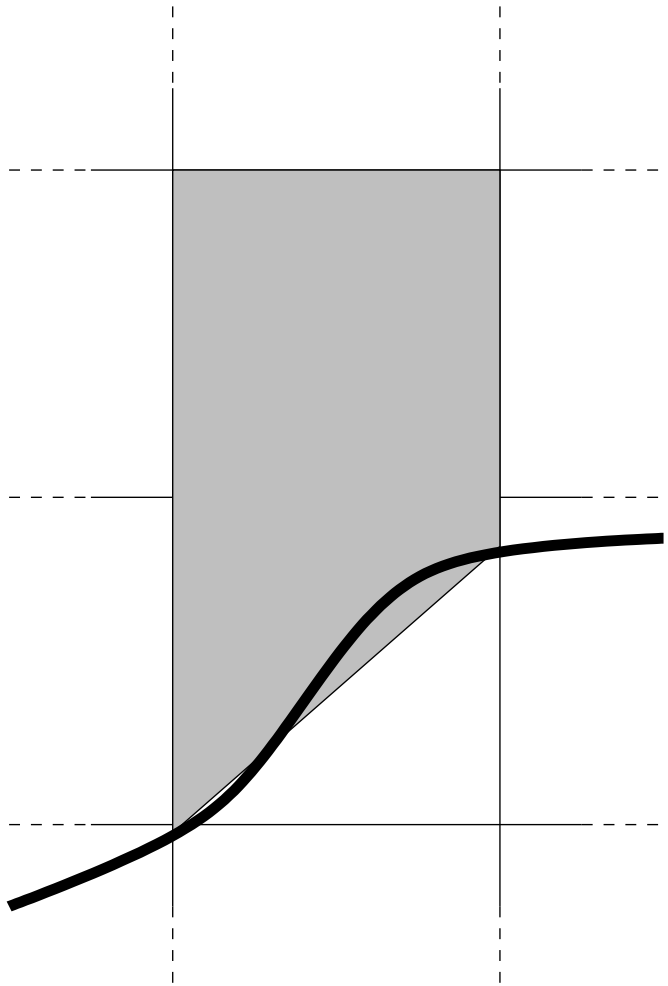

Technical details (I): small cell problem

- very small cut cells: very small Δt $\rightarrow$ cells merged in a control volume
- time integration in the control volume
- distribute the gas of the control volume to its cells :

$$\frac{1}{S^{n+1}} \int_{S^{n+1}} f \, \mathrm{d}S$$

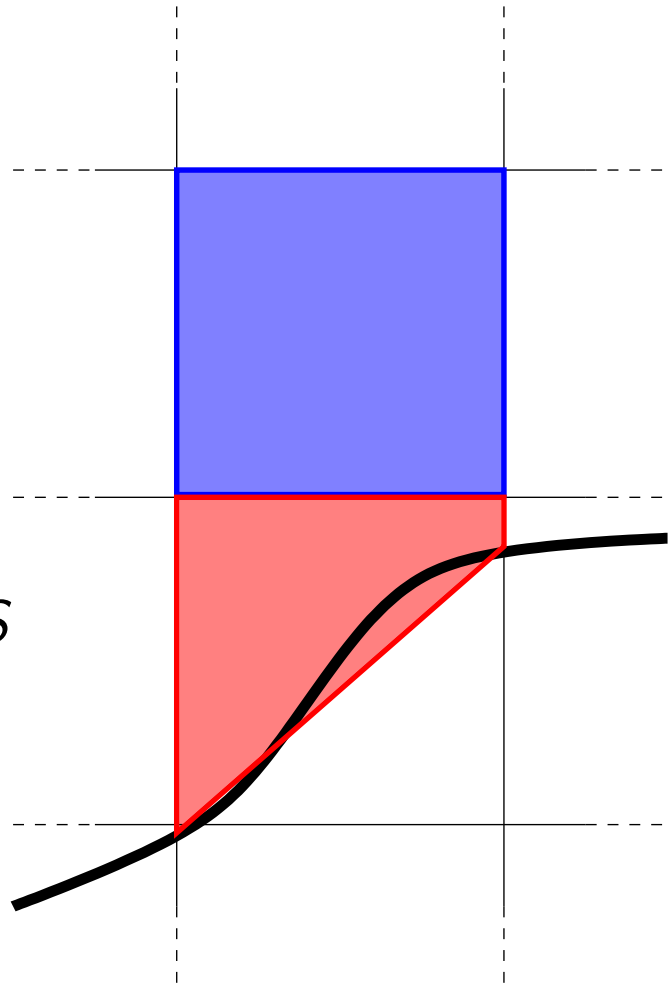

Technical details (I): small cell problem

- very small cut cells: very small Δt $\rightarrow$ cells merged in a control volume
- time integration in the control volume
- distribute the gas of the control volume to its cells :

$$\frac{1}{S_1^{n+1}} \int_{S_1^{n+1}} f \, \mathrm{d}S = \frac{1}{S^{n+1}} \int_{S^{n+1}} f \, \mathrm{d}S,$$

$$\frac{1}{S_2^{n+1}} \int_{S_2^{n+1}} f \, \mathrm{d}S = \frac{1}{S^{n+1}} \int_{S^{n+1}} f \, \mathrm{d}S.$$

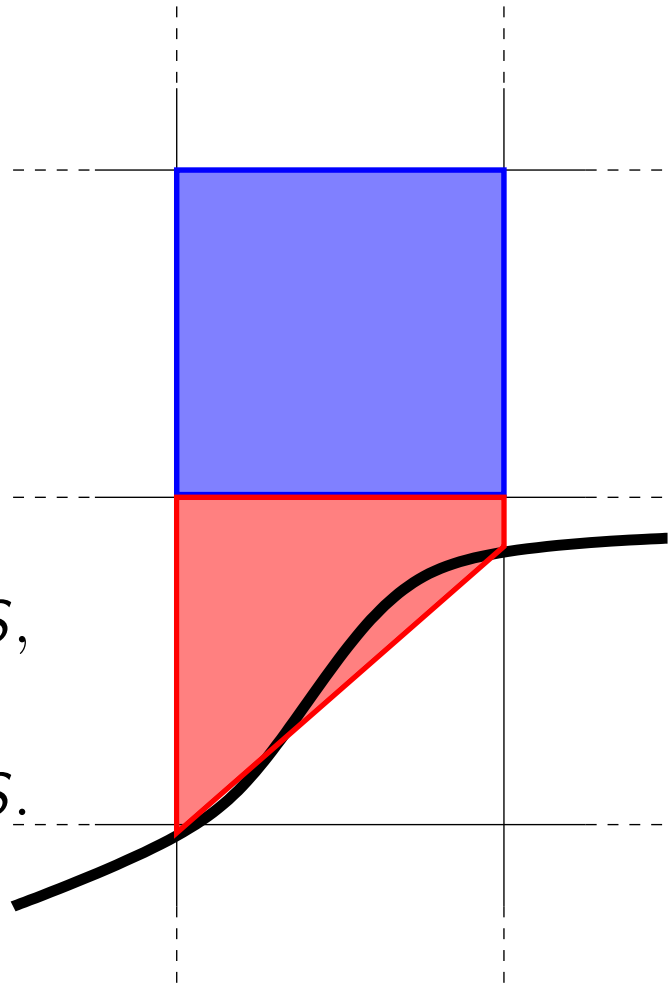

Technical details (II): disappearing cut-cells

- disappearing cut cell:

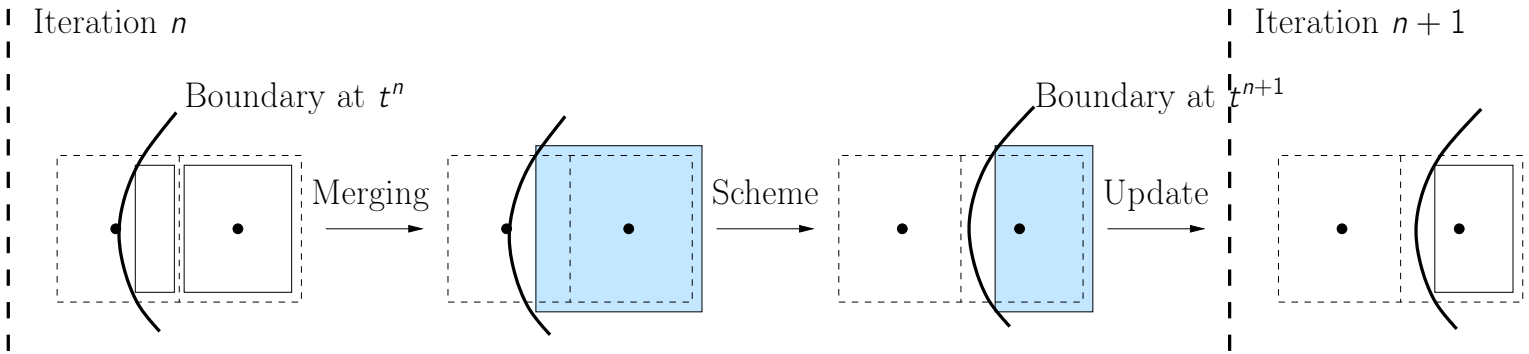

Technical details (II): appearing cut-cells

- appearing cut-cell:

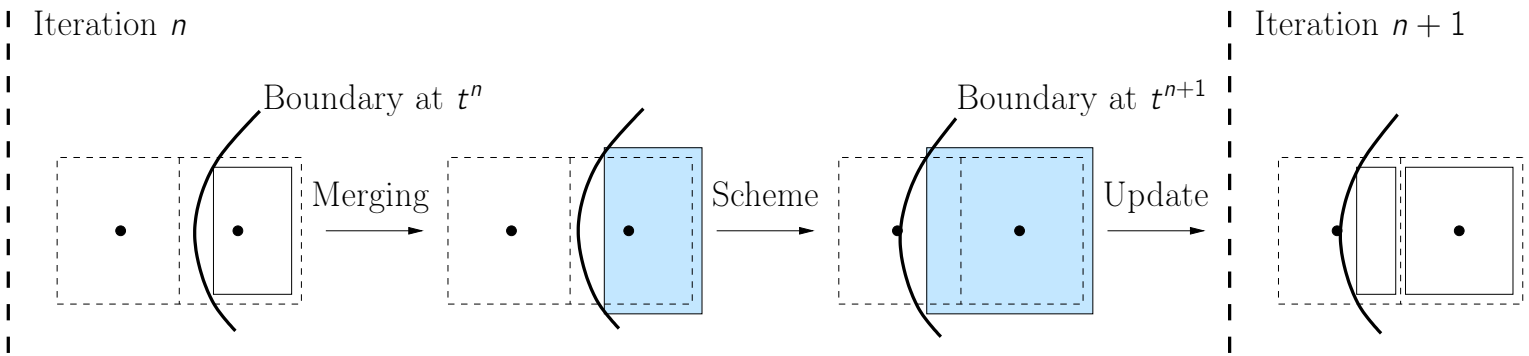

Properties

- stable: standard CFL condition
- exact mass conservation

Numerical results

- Simulations of Taguchi and Aoki [2012] :

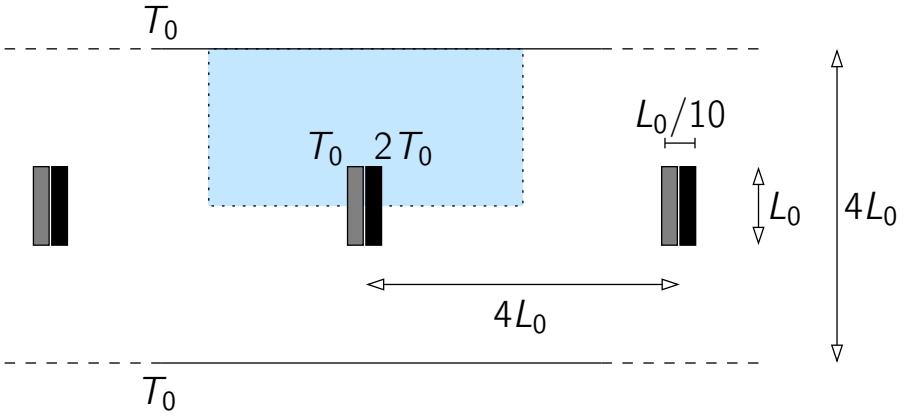

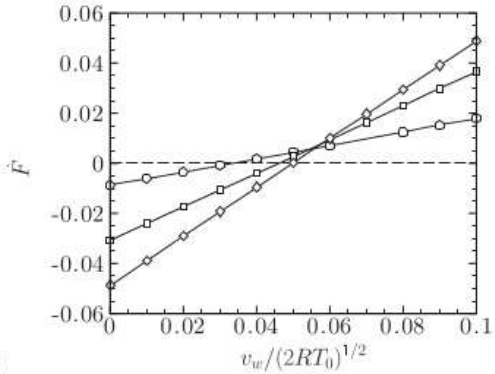

- Comparison with Taguchi and Aoki (steady case):

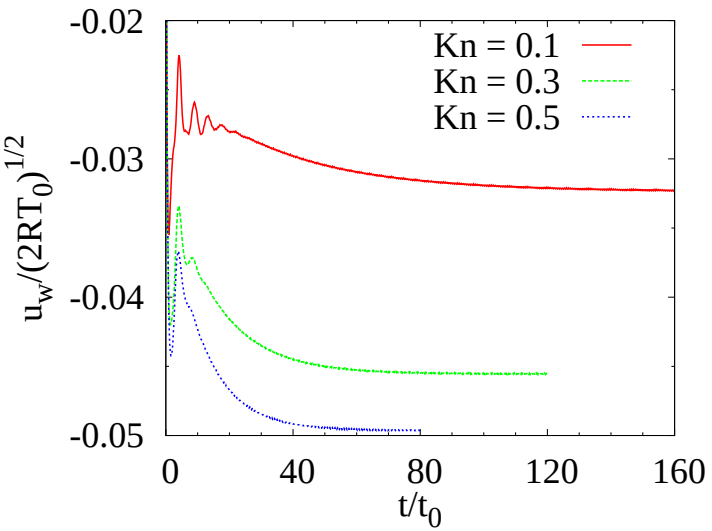

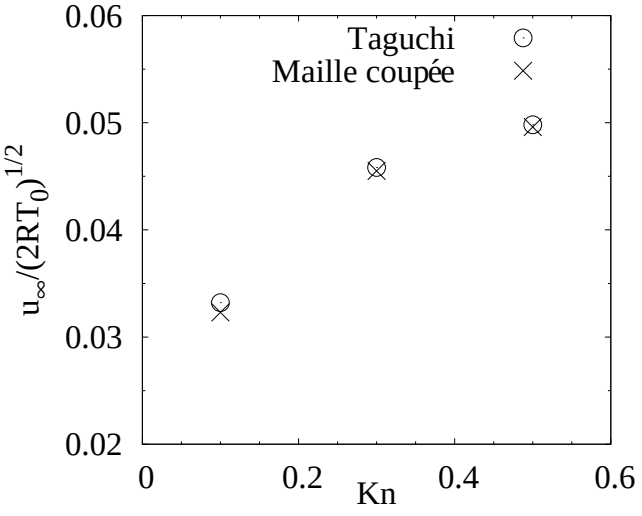

Numerical results

- Simulations of Taguchi and Aoki [2012] :

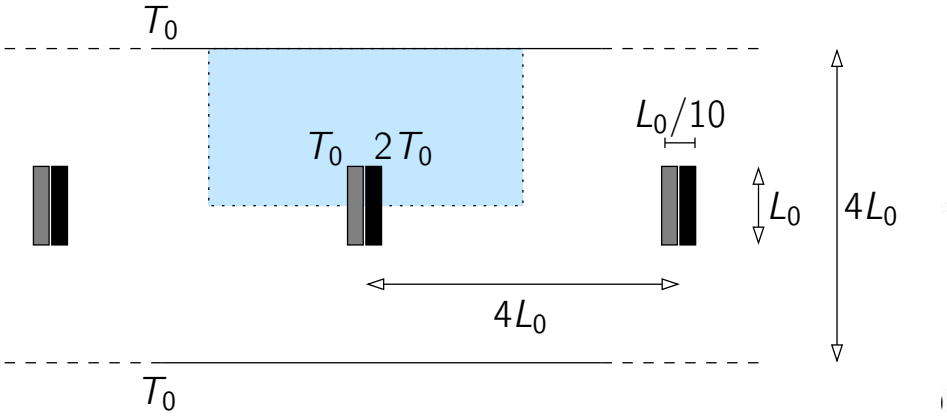

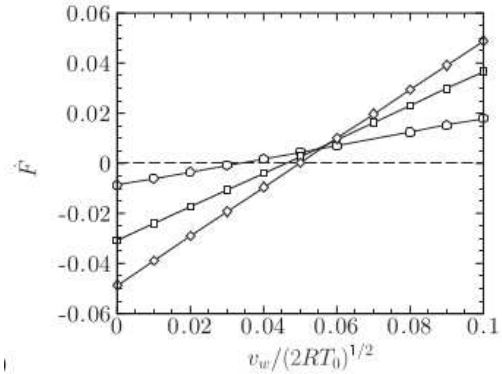

- Unsteady cut-cell simulation:

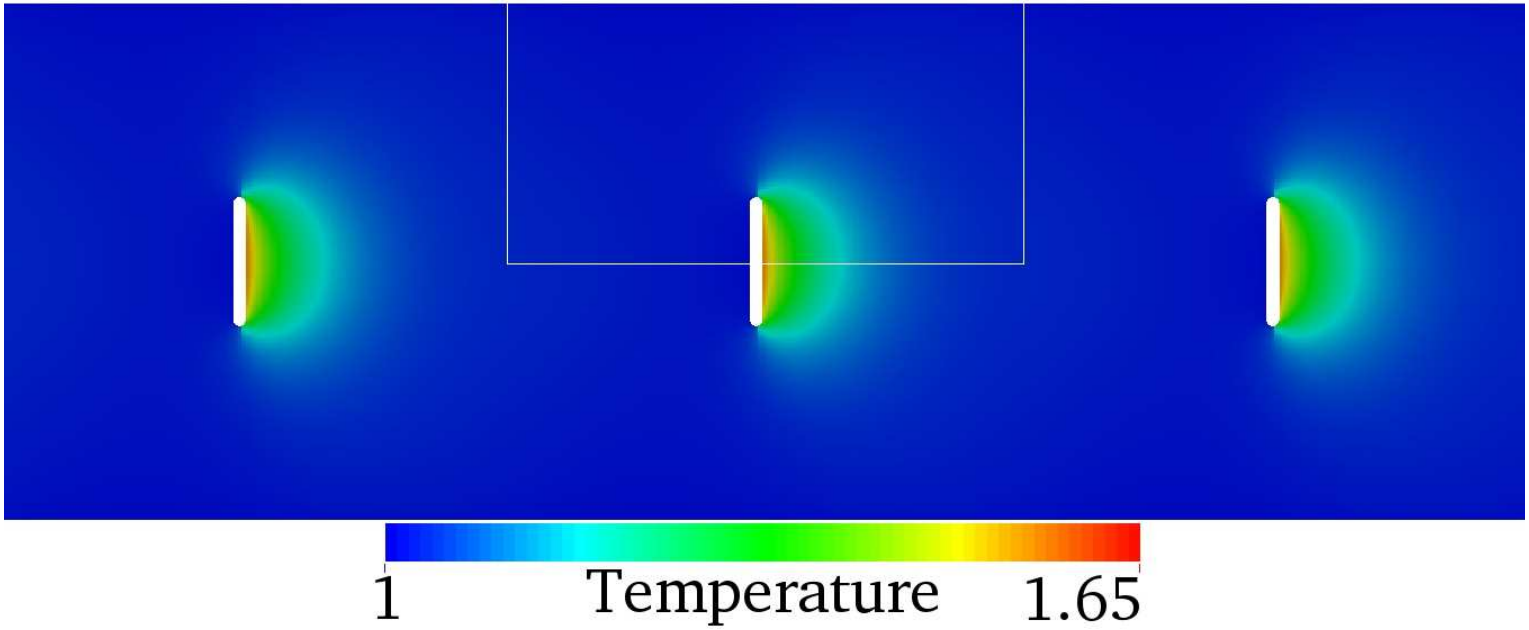

Numerical results

- Simulations of Taguchi and Aoki [2012] :

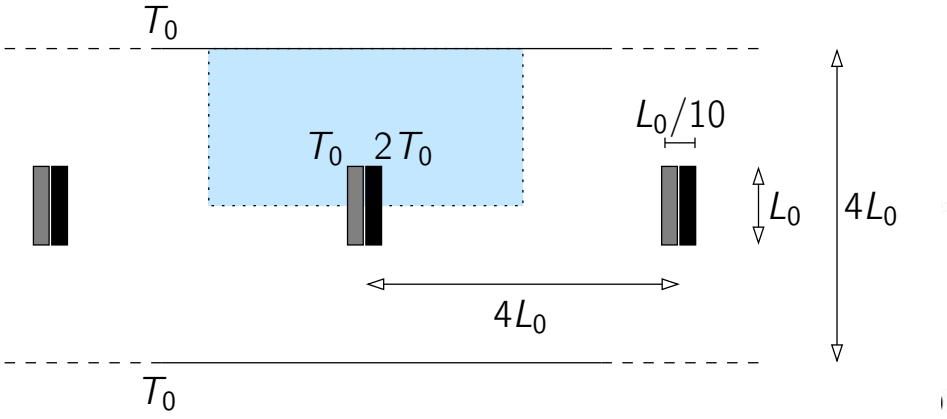

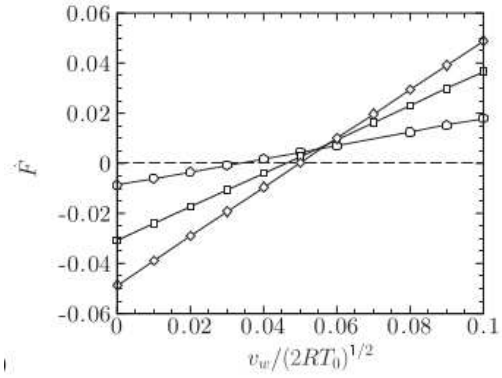

- Unsteady cut-cell simulation:

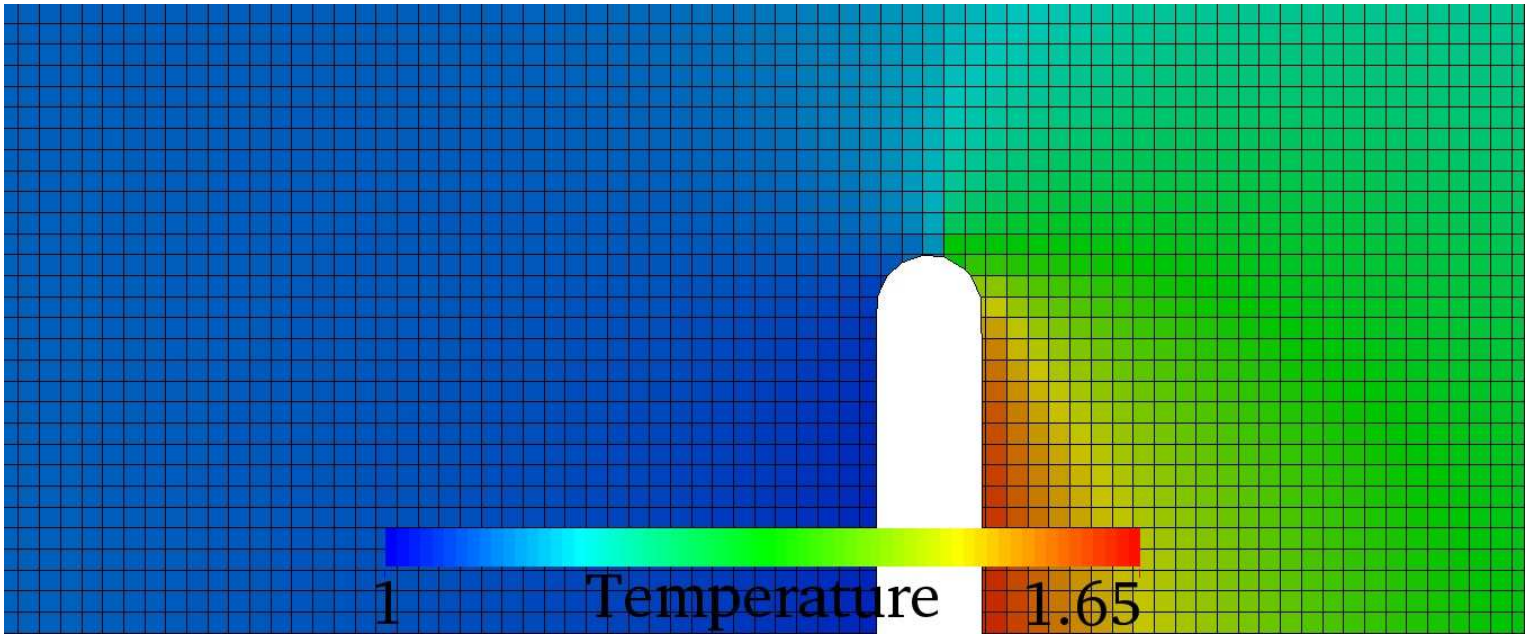

Numerical results

- Simulations of Taguchi and Aoki [2012] :

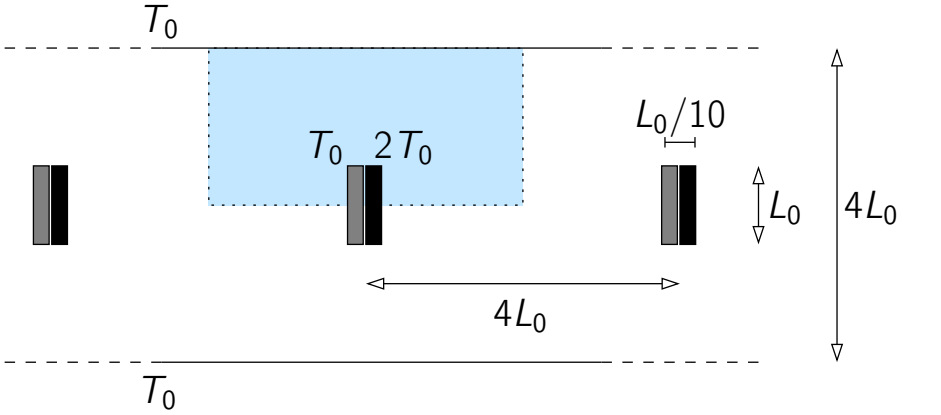

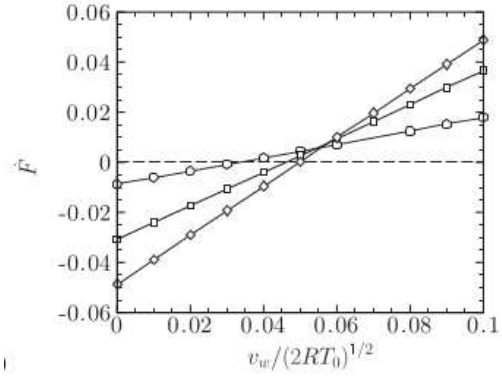

- Comparison with a body fitted unstructured mesh code (steady case):

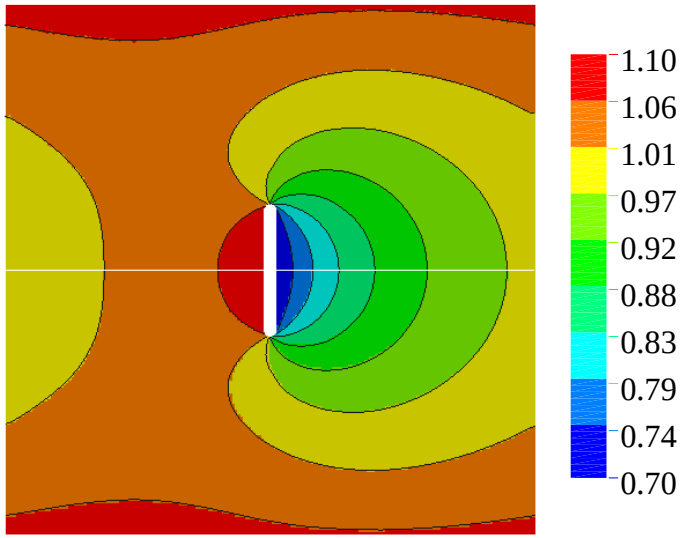

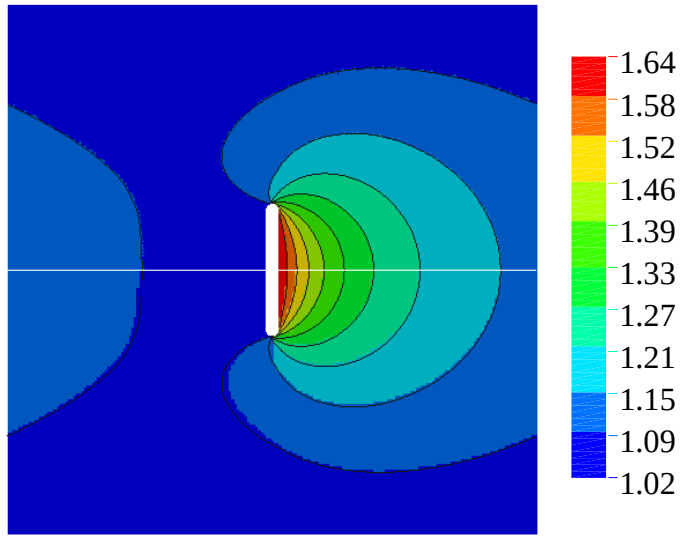

Numerical results

- 2D radiometer: comparison with Chen et al. (2012, moving mesh method)

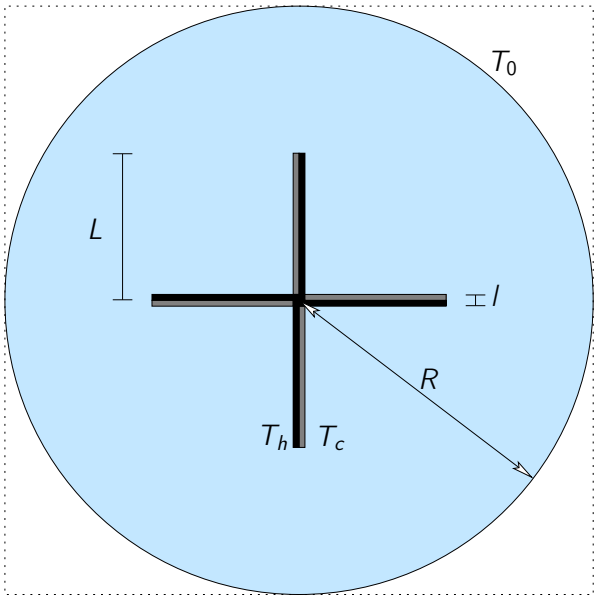

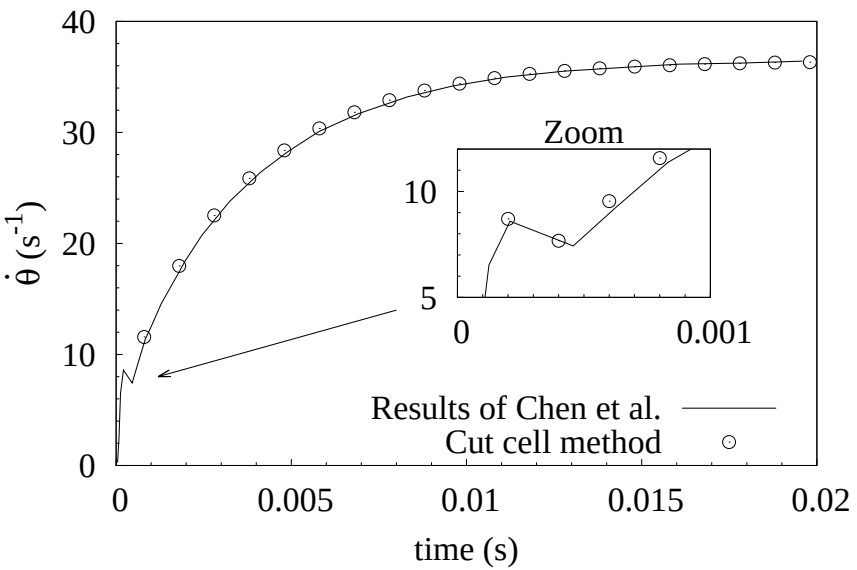

Numerical results

- Other application: vacuum pump (Roots pump)

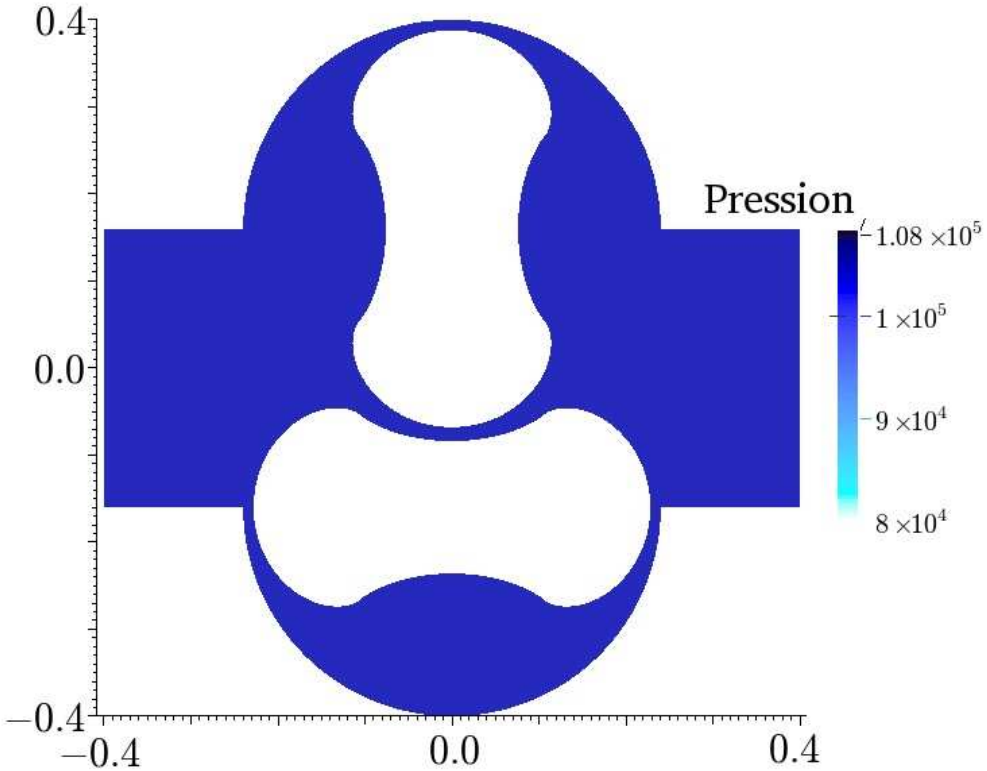

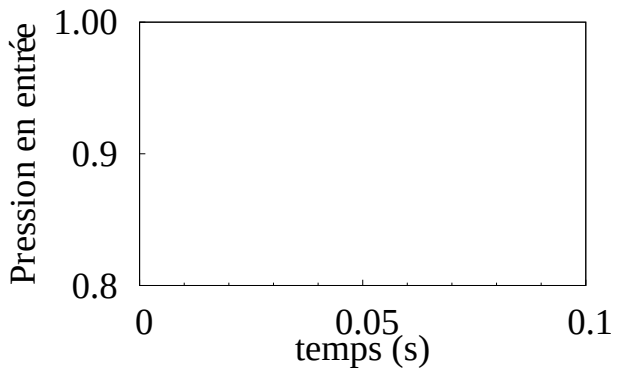

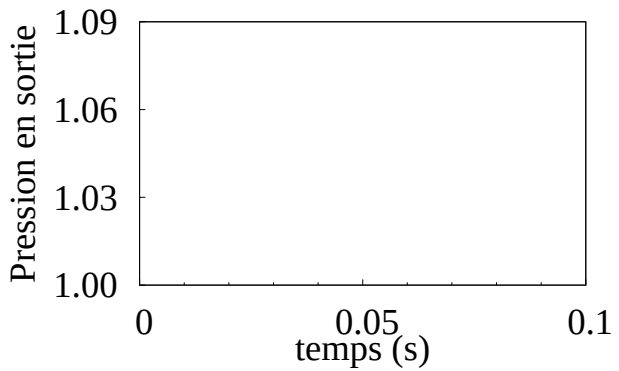

Numerical results

- Other application: vacuum pump (Roots pump)

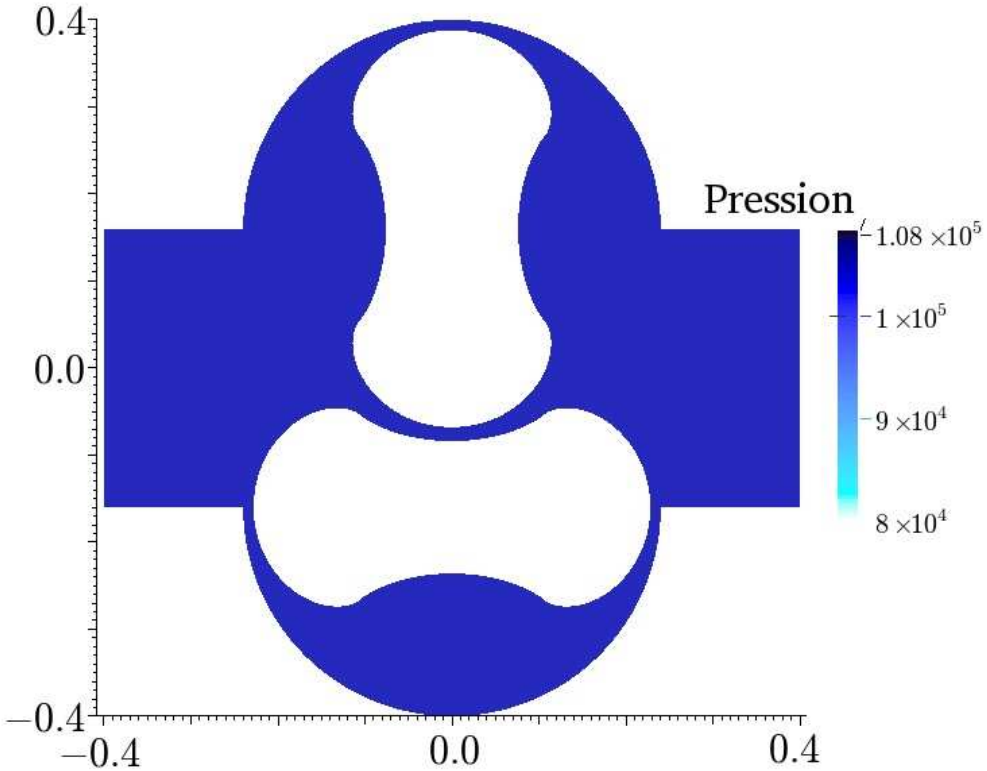

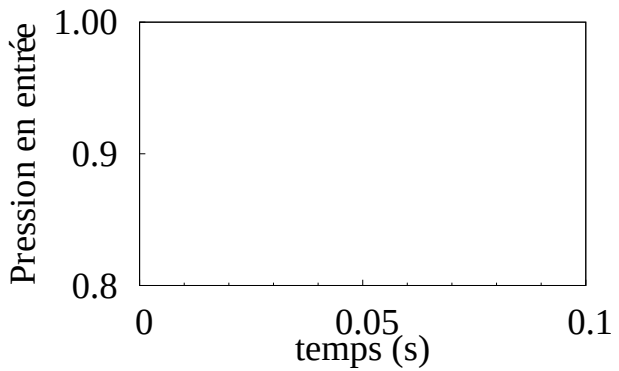

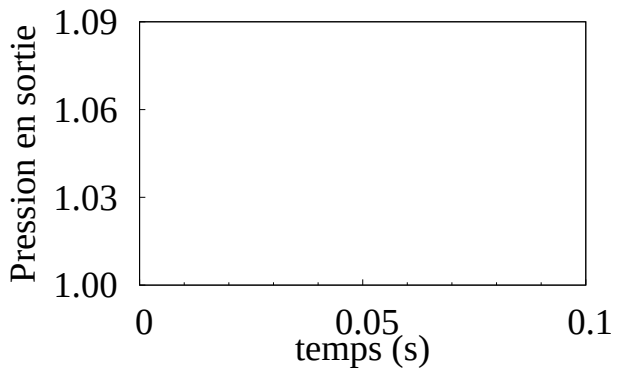

High performance computing (I): adaptive mesh refinement

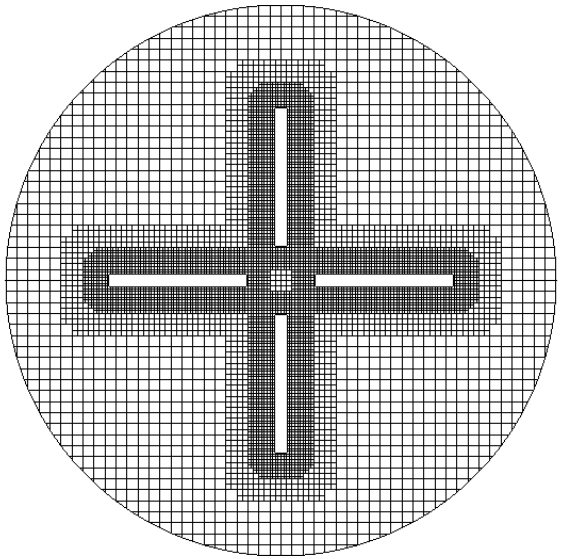

- Implementation of a **Quadtree** algorithm in space.
- Refinement criterion based on the **distance** between the cell and the nearest solid boundary.
- **Coupling** AMR - and the cut cell method is simple.

High performance computing (I): adaptive mesh refinement

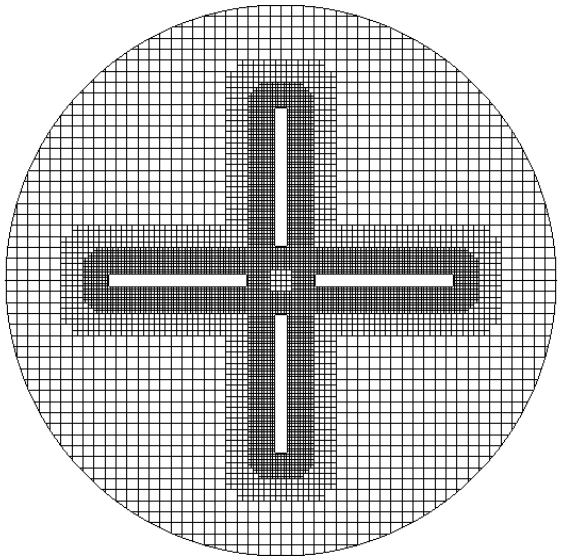

- Implementation of a **Quadtree** algorithm in space.
- Refinement criterion based on the **distance** between the cell and the nearest solid boundary.
- **Coupling** AMR - and the cut cell method is simple.

High performance computing (I): adaptive mesh refinement

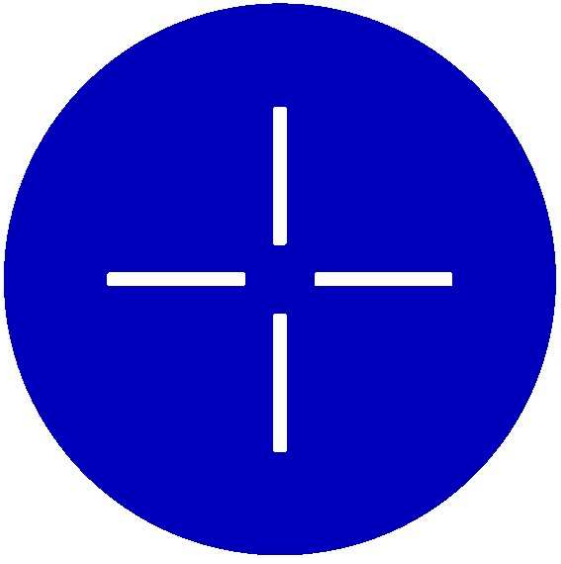

- Implementation of a **Quadtree** algorithm in space.
- Refinement criterion based on the **distance** between the cell and the nearest solid boundary.
- **Coupling** AMR - and the cut cell method is simple.

High performance computing (I): adaptive mesh refinement

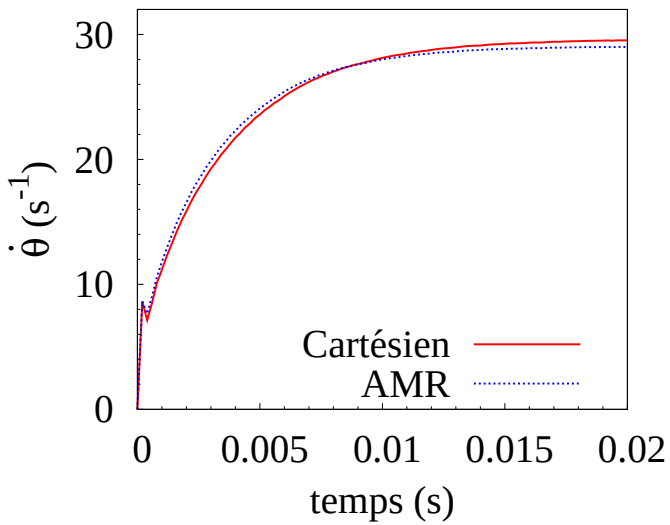

- Implementation of a **Quadtree** algorithm in space.
- Refinement criterion based on the **distance** between the cell and the nearest solid boundary.
- **Coupling** AMR - and the cut cell method is simple.

High performance computing (II): parallel implementation

- parallelization with MPI
- load balancing is difficult with moving boundaries
- hybrid domain decomposition in space and velocity :
  - a small number of subdomains in space
  - in each subdomain, the velocity grid is distributed to several processors
- this allows a good load balancing

3D implementation

How to treat all the different cut cells in a simple and single way?

- a normal cell is a cube (6 faces)
- a cut cell is a polyhedron with 4 to 7 faces

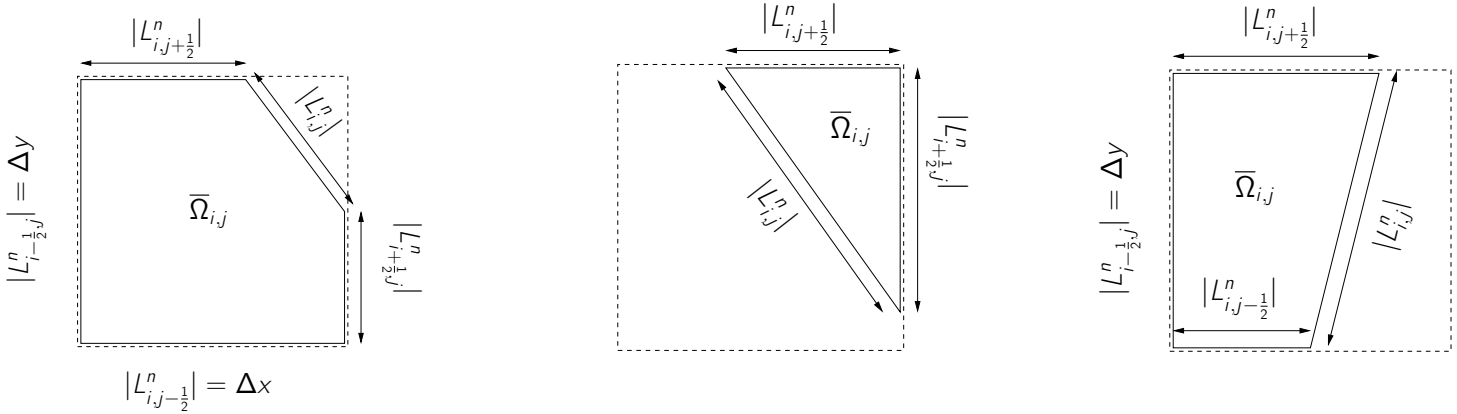

- notion of "virtual cell":
  - a virtual cell is a polyhedron with 7 faces, possibly degenerated
  - a virtual cell is associated to each cells
- generic treatment of every kind of cut cell
- passing from 2D to 3D is easy

Numerical Results

- 3D Radiometer:
  - ▷ 21^3 discrete velocities.
  - ▷ 240 000 cells (AMR).
  - ▷ 10 000 time steps.
  - $\rightarrow$ CPU time: 12h on 128 processors.

3D Simulation

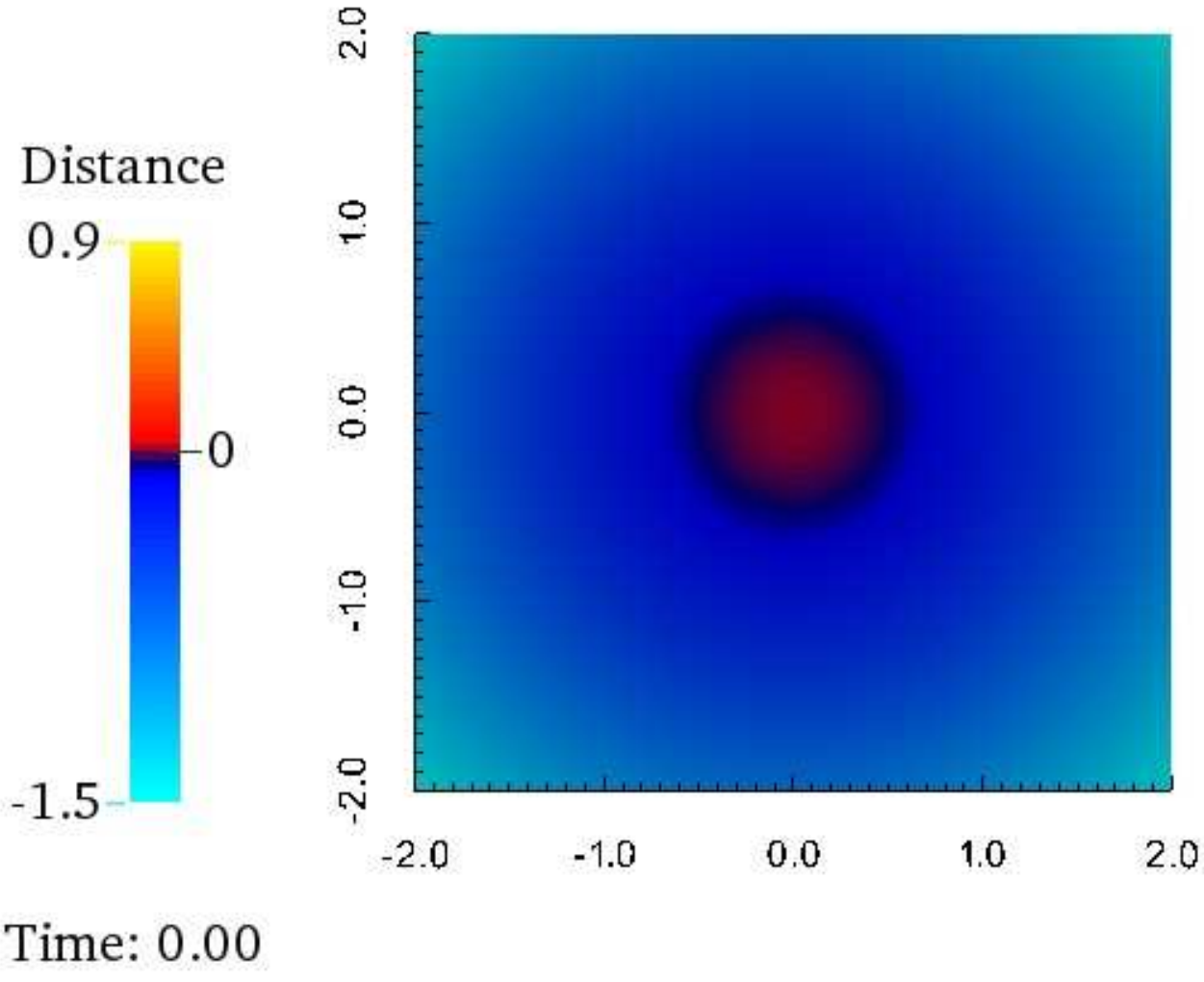

Conclusion

- Summary:
  - ▷ a general method to simulate rarefied flows with moving obstacles,
  - ▷ validation in 1 et 2 dimensions
  - ▷ general treatment of cut cells allows complex 3D simulations
- Perspectives:
  - ▷ might be useful for exploring radiometric effects, 3D flow structure, force magnitude and location
  - ▷ validation of the 3D code (experiments ?)
  - ▷ 2D free version available soon ("CAKE")